

Toward More Universal Prediction of Polymer Solution Viscosity for Solvent-Based Recycling

Rita Kol, Pieter Nachtergaele, Tobias De Somer, Dagmar R. D'hooge, Dimitris S. Achilias, and Steven De Meester*



Cite This: *Ind. Eng. Chem. Res.* 2022, 61, 10999–11011



Read Online

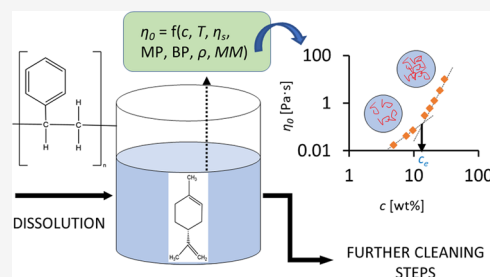
ACCESS |

Metrics & More

Article Recommendations

Supporting Information

ABSTRACT: The viscosity of polymer solutions is important for both polymer synthesis and recycling. Polymerization reactions can become hampered by diffusional limitations once a viscosity threshold is reached, and viscous solutions complicate the cleaning steps during the dissolution–precipitation technique. Available experimental data is limited, which is more severe for green solvents, justifying dedicated viscosity data recording and interpretation. In this work, a systematic study is therefore performed on the viscosity of polystyrene solutions, considering different concentrations, temperatures, and conventional and green solvents. The results show that for the shear rate range of $1\text{--}1000\text{ s}^{-1}$, the solutions with concentrations between 5 and 39 wt % display mainly Newtonian behavior, which is further confirmed by the applicability of the segment-based Eyring-NRTL and Eyring-mNRF models. Moreover, multivariate data analysis successfully predicts the viscosity of polystyrene solutions under different conditions. This approach will facilitate future data recording for other polymer–solvent combinations while minimizing experimental effort.



1. INTRODUCTION

The viscosity of polymer solutions is an important parameter in many processes, such as solution/bulk polymerization,^{1–3} as well as polymer recycling, especially in the field of solvent-based recycling.⁴ In solution polymerization, the viscosity can go significantly up at higher monomer conversions so that chemical phenomena are disturbed by diffusional limitations.² The same is true for solvent-based recycling purposes.

Solvent-based techniques can be categorized into two groups: solid–liquid extraction techniques and dissolution–precipitation technique.^{5,6} In the dissolution–precipitation technique, which is the focus of the present work, the polymer is dissolved in a suitable solvent, followed by one or more separation processes, e.g., filtration or centrifugation, to remove the contaminants. Finally, the addition of an antisolvent induces precipitation of the polymer.⁴ One of the advantages is the selective dissolution of polymers, especially important for multilayer materials recycling. For example, with the solvent-targeted recovery and precipitation (STRAP) strategy, Walker et al.⁷ recovered PE, ethylene vinyl alcohol, and PET from a postindustrial multilayer film. One of the crucial factors for the economic balance of the dissolution–precipitation technique is the concentration of the polymer solution. Low concentrated solutions lead to less viscous solutions but require high amounts of both solvent and antisolvent. The recommended polymer concentration for dissolution-based recycling is between 5 and 20 wt %, and the ratio of antisolvent/solvent is within 3:1 to 15:1.⁹ This means that for 1 kg of the polymer, 4–19 kg of solvent and a range of

12–285 kg of antisolvent are necessary.⁴ These high amounts of solvent increase the overall process cost and lower the sustainability character. On the other hand, a highly concentrated solution leads to very viscous solutions, which are difficult to handle during cleaning steps such as filtration.

Polymer solutions can also be characterized by three main regimes: a dilute, semi-dilute, and concentrated regime.⁴ In diluted solutions, the polymer chains behave as isolated hard spheres.¹⁰ It has been reported that typically polymer solutions are in this regime for (mass) concentrations lower than 5 wt %.^{11,12} The semi-dilute region can be subdivided into unentangled semi-dilute and entangled semi-dilute regimes (Figure 1a).^{11,13,14} In unentangled semi-dilute regime, the polymer chains are more tightly packed compared to the dilute regime, and in contact with each other, but there are no significant polymer chain entanglements.^{11,13} The entangled semi-dilute regime is then characterized by the presence of polymer chain entanglements,^{11,13} which considerably increases the viscosity of polymer solutions. In the concentrated regime, polymer chain entanglements dominate,^{10,15} and these entanglements are also shear-dependent.¹⁶ By plotting the dynamic viscosity as a function of polymer concentration on a

Received: April 28, 2022

Revised: June 27, 2022

Accepted: July 1, 2022

Published: July 14, 2022



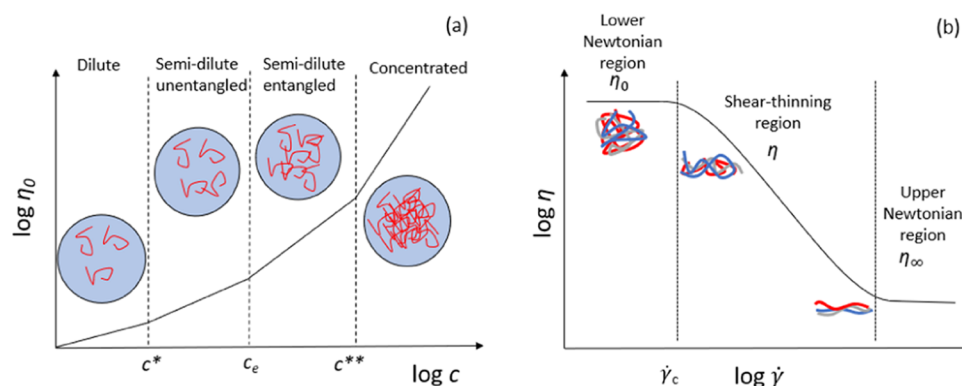


Figure 1. (a) Concentration regimes of polymer solutions. Blue colored circles represent the solution, and the red chains represent the polymer chains. Reprinted from Structural Study of a Polymer-Surfactant System in Dilute and Entangled Regime: Effect of High Concentrations of Surfactant and Polymer Molecular Weight, 1199, Afeni, A., Guettari, M., Kamli, M., Tajouri, T., Ponton, A., *J. Mol. Struct.*, 127052, Copyright (2020), with permission from Elsevier; (b) Typical viscosity flow curve of polymer solutions displaying shear-thinning. The different colors represent polymer chains, and $\dot{\gamma}_c$ is the shear rate defining the transition to shear-thinning. Reprinted from Kol et al.⁴

log–log scale, the critical concentrations that define the transition from one regime to another can be determined,^{11,17} where c^* is the (first) critical concentration, c_e is the entanglement concentration, and c^{**} is a second critical concentration (Figure 1a).^{10,13,17}

The knowledge and prediction of the rheology of polymer solutions thus play an important role for the optimization of polymerization and solvent-based recycling processes. The rheology of polymer solutions is inherently complex, as it depends on several factors, including the concentration of the polymer in solution, the average molar mass of the polymer, temperature, pressure, interaction of the solvent with the polymer, and polymer properties, such as configuration, dispersity, and branching level, among others.⁴ The viscosity flow curve of polymer solutions, similar to that of polymer melts, displays typically three regions (Figure 1b): (i) a lower Newtonian region at low shear rates, characterized by the zero-shear viscosity or Newtonian viscosity, η_0 , (ii) a shear-thinning region, and (iii) an upper Newtonian region, characterized by the infinite shear viscosity, η_∞ , which is difficult to reach experimentally.^{18,19} Similar to polymer melts, as the shear rate increases, the (linear) polymer chains start to align in the shear field and at very high shear rates; the chains are essentially aligned, resulting in much lower (dynamic) viscosities.^{4,19}

Several models have been proposed to describe the different regions of the viscosity flow curve of polymer solutions. These models are typically divided into Newtonian and non-Newtonian models. The (simplified) Newtonian models are a combination of Eyring's theory and local composition models to account for nonlinearity.⁴ The non-Newtonian models are empirical models proposed to describe the influence of shear rate on viscosity.¹² A frequently applied non-Newtonian model is the Ostwald–de Waele power-law model, which is able to describe the shear-thinning region. Other models, such as the Carreau and Cross model, can incorporate both the zero-shear and infinite shear viscosity, which make these models more suitable to predict the complete viscosity curve of polymer solutions.¹⁶ The application of these models in the field of solvent-based recycling can facilitate the competitiveness of this recycling route due to the importance of the viscosity of polymer solutions for the overall process. Yet, many of these models require dedicated experimental data recording of the different polymer–solvent combinations. For some polymer

solutions in conventional organic solvents, the Newtonian viscosity is reported in the literature, for example, for polystyrene (PS) for different solvents (e.g., styrene, toluene, and ethylbenzene) and concentrations,^{20,21} for poly(ethylene glycol) solutions,²² poly(vinyl chloride) solutions,²³ and low-density polyethylene solutions at high temperatures and pressures.^{24,25}

This dependency on extensive experimental data recording is a drawback for the direct application of common viscosity models. As an alternative, statistical approaches based on existing data can be used that can significantly reduce the need for new data and facilitate the developments in this field. For example, multivariate data analysis (MVA) has been applied in several sectors to reduce the dimensionality of data to simplify visualization and interpretation.²⁶ In MVA techniques, high-dimensionality data is reduced to low-dimensional data using linear combinations. These linear combinations are called principal components in the case of principal components analysis (PCA)²⁷ or latent variables in the case of partial least-squares (PLS) regression.²⁶ MVA has been applied to predict the viscosity and rheology of materials in different fields, e.g., for the prediction of the viscosity of crude oil,²⁸ the rheological behavior of fermentation broths²⁹ and pectin solutions,³⁰ and the rheological properties of polyacrylamide solutions,³¹ among others.^{32–34}

A key aspect is the selection of the solvent range, bearing in mind that there is a growing interest in shifting from “conventional” organic solvents to “green” solvents. Conventional solvents have high volatility, flammability, and toxicity.³⁵ For example, organic solvents such as toluene and benzene are good solvents for polystyrene, but these solvents may limit the further application of recycled plastic, e.g., in food packaging.³⁶ Additionally, some “green” solvents such as limonene have the advantage of minimizing molecular degradation during the recycling process,³⁶ which is an important factor to promote closed-loop recycling of plastics. Currently, production volumes of many green solvents are still low, but several strategies are being studied to increase the production volume of limonene for large-scale applicability.^{37–43} For many of these “green” solvents, no data is available on polymer solution viscosity, at least to our knowledge, hampering the use of models for proper design of recycling processes. Furthermore, solvent selection can be studied theoretically a priori based on

Table 1. Summary of the Solvent Properties and Hansen Solubility Parameters Reported at 25 °C, as well as the Final Experimental Findings^a

solvent	classification	MP [°C]	BP [°C]	MM [g·mol ⁻¹]	δ_D [MPa ^{1/2}]	δ_P [MPa ^{1/2}]	δ_H [MPa ^{1/2}]	R_a [MPa ^{1/2}]	RED	experimental screening at RT: dissolved?
<i>o</i> -xylene	aromatic (nonpolar)	-24	144	106.17	17.8	1.0	3.1	8.6	0.7	yes
<i>n</i> -butyl acetate	ester (aprotic)	-78	126	116.16	15.8	3.7	6.3	11.4	0.9	yes ^b
THF	ether (polar aprotic)	-108	65	72.11	17.8	5.7	8.0	7.9	0.6	yes
(<i>R</i>)-(+)-limonene	terpene (nonpolar)	-74	178	136.24	17.2	1.8	4.3	9.1	0.7	yes
geranyl acetate	terpenoid (aprotic)	<25	238	196.29	15.8	2.3	5.7	11.6	0.9	yes
cyclohexanol	alcohol (polar protic)	26	161	100.16	17.4	4.1	13.5	12.2	1.0	no
2-propanol	alcohol (polar protic)	-88	82	60.10	15.8	6.1	16.4	16.4	1.3	no
anisole	ether (polar aprotic)	-37	154	108.14	17.8	4.1	6.7	7.6	0.6	yes

^aAbbreviations: BP—boiling point, MP—melting point, MM—molar mass, R_a —distance in Hansen space, RED—relative energy difference value, RT—room temperature. Greek symbols: δ_D is the dispersion cohesion (solubility) parameter, δ_H is the hydrogen bonding cohesion (solubility) parameter, and δ_P is the polar cohesion (solubility) parameter. ^bCloudy solution at RT and 40 °C and transparent solution obtained at 50 °C.

the Hansen solubility parameters, molecular dynamics simulations, and combined quantum chemical and statistical mechanical approach called the conductor-like screening model (COSMOS-RS).^{7,44}

The objective of the present work is therefore to understand the viscosity flow curve of polystyrene solutions in nonpolar, polar protic, and polar aprotic solvents, addressing several temperatures and concentrations, which are important parameters for the dissolution–precipitation technique. Next to the conventional solvents *n*-butyl acetate, *o*-xylene, tetrahydrofuran, anisole, cyclohexanol, and 2-propanol, two “green” solvents, (*R*)-(+)-limonene and geranyl acetate, are included in this assessment. The typical viscosity models are applied to analyze which of them are the most promising for solvent-based recycling. Furthermore, an MVA-based model is developed, and the prediction of the viscosity of polystyrene solutions with this new model is evaluated.

2. MATERIALS AND METHODS

2.1. Materials. Polystyrene pellets (Styron 634-71) were purchased from Resinex. As provided by the supplier, the mass average molar mass, M_w , is 265 000 g·mol⁻¹, and the dispersity of the molar mass distribution, D , is 2.65. Five solvents were chosen to study the influence of the solvent type on the rheology of the polymer solutions. The choice of the solvents was based on their properties, such as molecular structure, melting and boiling point, viscosity, and toxicity. These solvents include *n*-butyl acetate (99% purity, Alfa Aesar), *o*-xylene (99% purity, Alfa Aesar), tetrahydrofuran (99% purity, Sigma-Aldrich, Merck), anisole (99% purity, Sigma-Aldrich, Merck), cyclohexanol (99% purity, Chem-Lab), and 2-propanol (99.8% purity, Chem-Lab). Two “green” solvents, (*R*)-(+)-limonene (93% purity, Sigma-Aldrich, Merck) and geranyl acetate (90% purity, Sigma-Aldrich, Merck) are included as well. The solvents were used as-received, without any purification.

2.2. Screening of Solvents toward Sufficient Polymer Solubility. The first screening of suitable solvents for polystyrene was done theoretically, based on reported Hansen solubility parameters (HSP).⁴⁴ To apply the HSP analysis, the relative energy difference (RED) value was calculated

(Supporting Information, Section 1). The RED number indicates the affinity between the polymer and the solvent. A RED value smaller than 1 indicates that the polymer and solvent have a high affinity, meaning that the solvent will likely dissolve the polymer.⁴⁴ Table 1 summarizes the solvent classifications, properties, HSP, and the calculated R_a and RED values. The RED values are all below 1, except for the alcohols, indicating that the polymer should dissolve in these solvents. By plotting δ_P vs δ_H in Figure 2, it follows that most solvents are within the Hansen sphere, R_o , which means that the solvents will likely dissolve PS.

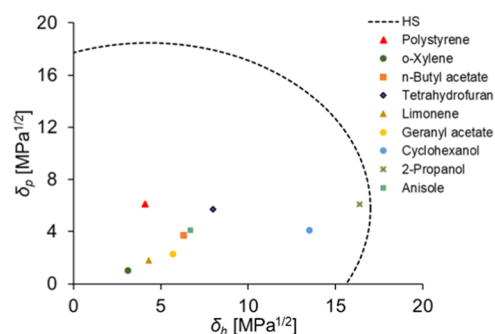


Figure 2. δ_P vs δ_H for polystyrene. Abbreviation: HS: Hansen sphere (2D projection).

To validate these results, an experimental screening was performed, which showed that all solvents dissolve polystyrene at room temperature (RT), apart from the alcohols (Table 1). In the case of ester (*n*-butyl acetate), the solutions are cloudy at room temperature. Based on these results, the final solvent choice for the analysis of viscosity is *o*-xylene, *n*-butyl acetate, THF, limonene, geranyl acetate, and anisole.

2.3. Solubility Determination. After the screening of the solvents, the solubility of polystyrene in the solvents *o*-xylene, *n*-butyl acetate, THF, limonene, geranyl acetate, and anisole was determined. Solutions were prepared by adding a known amount of solvent to a known amount of excess solute (polymer).⁴⁵ The samples were left sealed at room temperature for 1 week before measuring the concentration of the

obtained saturated solution with thermogravimetric analysis (TGA).⁴⁵ This TGA was conducted in a Netsch TG 209 F3 Tarsus thermogravimeter, and the measurements were carried out under a constant flow of dry nitrogen (N₂) at a rate of 20 mL·min⁻¹. The temperature profile was as follows: increase of temperature from 25 to 700 °C with a heating rate of 10 °C·min⁻¹. To ensure reproducibility, the measurement was performed three times for each sample. The error associated with the determination of polymer concentration with TGA was calculated, being less than 0.3 wt % (Supporting Information, Section 2).

2.4. Rheology. **2.4.1. Solvents.** An Ubbelohde capillary viscometer (Schott Instruments-CT 1450) was used to measure the kinematic viscosity of the solvents at different temperatures (20, 25, 40, and 50 °C). The capillary with the number 0C, which is suitable for samples with a kinematic viscosity range between 0.5–3 mm²·s⁻¹, was used for all solvents at all temperatures. To convert the kinematic viscosity to dynamic viscosity, the density of the solvents was measured with a pycnometer at the four different temperatures. The calibration of the pycnometer was performed at each temperature with distilled water. The pycnometer was left for 3 min in the thermostatic bath (Schott Instruments-CT 1450) at the desired temperature and then weighted using an analytical balance (Precisa-XR 205SM-DR, *d* = 0.01/0.1 mg). To ensure reproducibility, the measurements with the viscometer and pycnometer were carried out three times each, and the mean values together with the standard deviation are reported (Supporting Spreadsheet, Sheet 1).

2.4.2. Polystyrene Melt. Disk samples of pure polystyrene were prepared using a hot press Fontjne Holland. A mold with 25 mm circles was used. Before pressing, the samples were left on the hot press at 230 °C for 5 min to ensure the melting of the polymer, and then the samples were pressed under a pressure of 50 kN for 5 min. The viscosity of the polymer melt was measured using an Anton Paar rheometer MCR 702 Multidrive equipped with a CTD 600 MDR chamber. A 0.25 mm parallel plate geometry was used with a gap of 1 mm. The viscosity was measured at temperatures between 200 and 310 °C in a shear rate range between 0.01 and 30 s⁻¹. The measurements were carried out three times to ensure reproducibility, and all mean values are reported in the Supporting Spreadsheet (Sheet 1).

2.4.3. Polymer Solutions. Polystyrene was dissolved in the different solvents at concentrations ranging from 5 to 39 wt % at room temperature, depending on the solubility. Prior to the viscosity measurements, the solutions were placed in a heating bath at the temperature of the viscosity determination and stirred with a magnetic stirrer for a minimum of 5 min before the measurements. The viscosity of the polymer solutions was measured using a rotational rheometer (Anton Paar Rheometer MCR 702 Multidrive) with a 0.5 mm parallel plate geometry and a 0.5 mm gap. The viscosities were measured at different temperatures, namely 25, 40, and 50 °C, in a shear rate range between 1 and 1000 s⁻¹. To prevent solvent boiling and polymer degradation, temperatures higher than 50 °C were avoided,⁴⁶ and the same set of temperatures was then applied on all solutions. A solvent trap was used to prevent solvent evaporation during the measurement. For PS/THF solutions, the measurement of the viscosity was only possible at 20 °C due to the high volatility of the solvent. A transient test, i.e., measurement of the viscosity over time at a fixed shear rate, was also performed to better understand the

steady-state behavior of the samples at different shear rates. All experiments were performed three times to ensure reproducibility, and the mean value is reported with the standard deviation in the Supporting Spreadsheet (Sheets 2–7).

2.5. Modeling. **2.5.1. Newtonian Viscosity Models.** The Newtonian viscosity models proposed in the literature applicable to polymer solutions are summarized in Table S2 of the Supporting Information. A more detailed analysis of these models can be found in Kol et al.⁴ The segment-based Eyring-NRTL, Eyring-Wilson, Eyring-NRF, and modified-NRF are based on Eyring's theory and local composition models,⁴ whereas the polymer mixture viscosity model is based on the ideal linear mixing rule for polymer solutions and the nonideal mixing effect is described by a symmetric and anti-symmetric binary parameter.^{1,4}

The Newtonian viscosity models require the viscosity of the pure components as input. This study is based on binary mixtures, the pure components being the solvent and the polymer. If the viscosity of the pure components is unavailable, it can be either treated as an adjustable parameter or, in the case of polymer melts, it can be obtained using a modified Mark–Houwink equation:^{1,4,47–50}

$$\eta_0 = \eta_{\text{ref}} (M_w/M_{w,\text{ref}})^\alpha e^{[E_\eta/R(1/T - 1/T_{\text{ref}})]} \quad (1)$$

where η_0 is the Newtonian viscosity [Pa·s], η_{ref} is a reference viscosity [Pa·s], M_w is the mass average molar mass [g·mol⁻¹], $M_{w,\text{ref}}$ is the mass average molar mass of reference [g·mol⁻¹], E_η is the activation energy of viscous flow [J·mol⁻¹], R is the gas constant [J·K⁻¹·mol⁻¹], T is the temperature [K], and T_{ref} is the reference temperature [K].

For the solvents, the viscosity can be taken from literature or experimentally determined. In this work, the viscosity of the solvents was experimentally determined at different temperatures, and the viscosity of the polymer melt at low temperatures (25–50 °C) was estimated using the modified Mark–Houwink equation, following the methodology proposed by Song et al.¹ This extrapolation is physically not realistic, but the goal is to minimize the number of adjustable parameters in the model and avoid overfitting.

The model parameters in the Newtonian viscosity models were regressed by minimizing the sum of squares (SSE)

$$\text{SSE} = \sum_{i=1}^n (\log(\eta_{0,i}^{\text{exp}}) - \log(\eta_{0,i}^{\text{cal}}))^2 \quad (2)$$

where $\eta_{0,i}^{\text{exp}}$ is the experimental Newtonian viscosity value and $\eta_{0,i}^{\text{cal}}$ is the calculated value.

The evaluation of the performance of the model was done by analyzing the average relative error (ARE), absolute average relative deviation (AARD), Theil's inequality coefficient (TIC), chi-squared test (Chi), and hybrid fractional error function (HYBRID). The respective functions can be found in the Supporting Information (Table S3). The modeling was performed by nonlinear regression using an in-house-made script in R based on the Flexible Modeling Environment (FME) package. The SSE was minimized by the ModFit function in combination with a pseudorandom-search algorithm for parameter regression.

2.5.2. Multivariate Data Analysis. Multivariate analysis (MVA) techniques were applied to gain further insight into the effect of solvent properties, temperature, and concentration on the viscosity of polymer solutions. The MVA techniques were

applied following the systematic multivariate analysis (sMVA) strategy.²⁶

First, an exploratory principal component analysis (PCA) was performed on the main experimental data. The data contains the Newtonian viscosity of PS solutions for six solvents (geranyl acetate, limonene, *o*-xylene, *n*-butyl acetate, THF, and anisole), with concentrations between 5 and 39 wt % and temperatures between 20 and 50 °C at a shear rate of 10 s⁻¹, except for PS/*n*-butyl acetate, with data for 5 and 8 wt % at 40 °C at 19 s⁻¹. Based on this PCA analysis, a list of independent variables is selected for regression analysis.

Second, a partial least-squares (PLS) regression model is built and used to predict the viscosity of PS solutions. PLS considers the covariance between the independent variables and the dependent variables and is the most commonly used multivariate analysis technique for regression.⁵¹ The dependent variable, which the model attempts to predict, is the natural logarithm of the viscosity of PS solutions. The independent variables are a selection of solvent properties (e.g., solvent viscosity), properties regarding the affinity between the polymer and the solvent (e.g., RED), temperature, and concentration of the polymer in the solution. The model is validated using an external data set from literature. The validation data set contains PS solutions in styrene with concentrations between 6 and 32% at 30 °C.²⁰

The number of valuable latent variables (LV) to include in a PCA or PLS model depends on the complexity of the relation between the dependent and independent variables and the signal-to-noise ratio. Cross-validation (CV, Venetian blinds) was used to detect possible overfitting. CV is a model validation technique indicating how well the model would perform on new data by evaluating the model performance for different calibration–validation splits.⁵² The root-mean-square error of cross-validation (RMSECV) and the cross-validated coefficient of determination (R_{CV}^2) were used for selecting the number of principal components (PCs) or latent variables (LVs) used in the model.⁵³ The root-mean-square error of prediction (RMSEP) is employed for evaluating the model performance.⁵⁴ The RMSEP summarizes the overall error of the model for predicting the viscosity of PS solutions of a new solvent. The coefficient of determination R^2 and RMSE functions can be found in the Supporting Information (Table S3). Because PCA and PLS models are not scale-invariant, the data was mean-centered, and all variables were scaled to unit variance before analysis.⁵⁵ For comparison, the PLS regression results are compared to regression via multiple linear regression (MLR) using polymer concentration, temperature, and/or solvent density as input variables. The analyses were performed using the Eigenvector PLS_Toolbox 8.6.2 for MATLAB (R2018a).

3. RESULTS AND DISCUSSION

3.1. Solubility Limits of Polymer Solutions. To determine the maximal concentration of the solutions for reliable viscosity measurements, thermogravimetric analysis (TGA) curves of several polymer solutions were compared to the TGA curve of pure polystyrene (Supporting Information, Section 4). The solubility values of polystyrene in the different solvents are reported in Table 2. The results show that the solubility depends on the solvent, with *n*-butyl acetate having the highest solubility value of 62.7 wt %, followed by THF, anisole, *o*-xylene, limonene, and geranyl acetate. Note that with the solubility determination method, i.e., adding an excess

Table 2. Solubility Limit of Polystyrene in the Different Solvents at Room Temperature and Entanglement Concentrations, c_e

solution	PS solubility limit [wt %]	entanglement concentration [wt %]			
		temperature			
		20 °C	25 °C	40 °C	50 °C
PS/ <i>o</i> -xylene	53.9 ± 1.0		13.9	14.1	14.6
PS/ <i>n</i> -butyl acetate	62.7 ± 1.2		13.6	13.5	13.4
PS/THF	57.0 ± 0.2	13.0			
PS/limonene	47.1 ± 0.4		13.6	13.5	13.3
PS/geranyl acetate	40.9 ± 0.1		12.8	12.9	13.0
PS/anisole	58.5 ± 0.7		13.9	13.8	14.0

amount of polymer and measuring the concentration of the clearly saturated viscous solution, the regime of concentrated polymer solutions is reached, where entanglements are present. In this work, the goal is to determine the viscosity of polystyrene solutions at different (mass) concentrations, regardless of the regime, but still, it is important to ensure that the solution is below the solubility value and no undissolved polymer pellets are present during the viscosity measurements.

3.2. Viscosity of the Pure Solvent and the Polymer.

The viscosity of the pure solvents was determined to input them in the Newtonian viscosity models for the solutions. The dynamic (Newtonian) viscosity and the density of the solvents are present in the Supporting Spreadsheet (Sheet 1). *n*-Butyl acetate has the lowest dynamic viscosity at 25, 40, and 50 °C, followed by *o*-xylene, limonene, anisole, and geranyl acetate.

The viscosity curve of pure polystyrene melt (200–310 °C) displays mainly Newtonian behavior in the studied shear rate range of 0.01 and 30 s⁻¹ (Supporting Spreadsheet, Sheet 1). The Newtonian behavior is followed by shear-thinning behavior at higher shear rates. The critical shear rate, i.e., the shear rate that characterizes the transition from Newtonian to non-Newtonian behavior, shifts to higher shear rates as the temperature increases, which is coherent with the literature.¹² For the modeling, the Newtonian viscosity at 0.01 s⁻¹ was used.

3.3. Viscosity of Polymer Solutions. **3.3.1. Influence of Concentration.** The viscosity curves of the studied polymer solutions at 25 °C are presented in Figure 3. The results show that the higher the polymer concentration (but below the solubility limit), the higher the viscosity of the solution. This is an expected result, since the higher the concentration of the polymer solution, the more polymer chains are present in solution, which increases the resistance to the flow. The results show that the polymer solutions display mainly Newtonian behavior in the studied shear rate range of 1–1000 s⁻¹. Only at higher concentrations, e.g., at 30 wt % for PS/*o*-xylene solution and PS/limonene, 25 wt % for PS/*n*-butyl acetate, and 21 wt % for PS/geranyl acetate and PS/anisole, the viscosity curve starts to display non-Newtonian behavior. At a molecular level, long polymer chains in concentrated solutions interpenetrate extensively, which results in chain entanglements and topological constraints. This limits the polymer motion and consequently affects the flow properties by increasing the viscosity and resulting in shear-thinning behavior.^{56,57} The flow curve at higher temperatures displayed the same behavior and

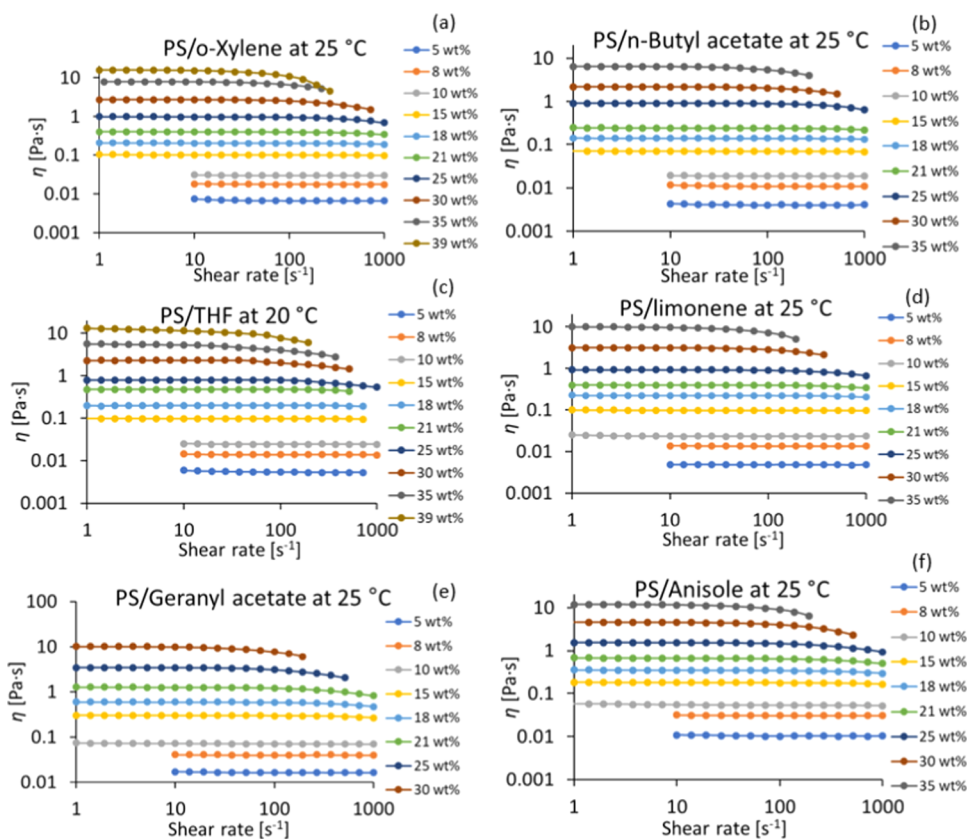


Figure 3. Influence of concentration on the viscosity of the polymer solutions—(a) PS/*o*-xylene solution at 25 °C; (b) PS/*n*-butyl acetate at 25 °C; (c) PS/THF at 20 °C; (d) PS/limonene at 25 °C; (e) PS/geranyl acetate at 25 °C, and (f) PS/anisole at 25 °C.

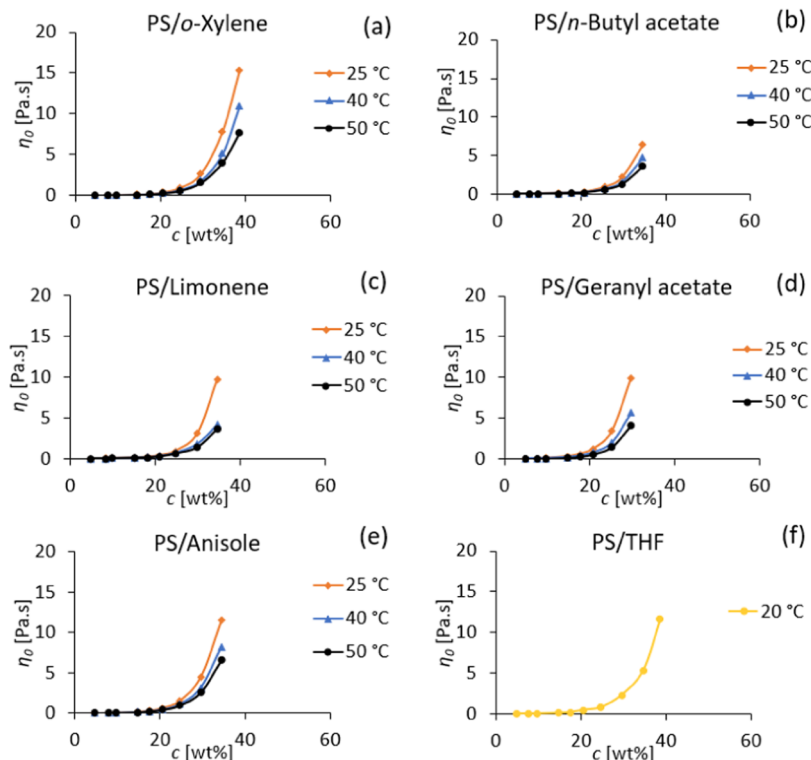


Figure 4. Newtonian viscosity, fixed at 10 s^{-1} , as a function of concentration at different temperatures and solvents—(a) PS/*o*-xylene, (b) PS/*n*-butyl acetate, (c) PS/limonene, (d) PS/geranyl acetate, (e) PS/anisole, and (f) PS/THF. *Except for PS/*n*-butyl acetate 5 and 8 wt % at 40 °C, which instead is 19 s^{-1} .

can be found in the Supporting Spreadsheet (Sheets 2–7). These results are relevant for solvent-based recycling, especially for solid–liquid separation processes, where expected shear rate ranges are 10^{-4} – 10 s^{-1} for colloidal filtration and 1 – 100 s^{-1} for the belt filter press.⁵⁸

A transition test was performed as well to study the steady-state behavior of the solutions. In fact, for low concentration, the viscosity is only stable above 10 s^{-1} , and for high concentration, only up to 300 s^{-1} on average. Further information can be found in the Supporting Information (Figures S11–S23).

3.3.2. Influence of Temperature. The influence of temperature on the shear-thinning behavior of highly concentrated solutions of polystyrene (>30 wt %) shows that higher temperatures decrease the viscosity and the shear-thinning behavior of the polymer solutions as the critical shear rate moves to higher shear rates (Supporting Information, Figure S24).

Furthermore, the flow behavior of lower concentrated polymer solutions, i.e., from 5 to 20 wt % displays mainly Newtonian behavior in the studied shear rate range. Figure 4 displays the Newtonian viscosity as a function of concentration at different temperatures. Above a certain concentration, between 13 and 15 wt % on average, the Newtonian viscosity even increases drastically and follows a power-law behavior. This concentration is referred to as entanglement concentration c_e and defines the transition from a semi-dilute unentangled to a semi-dilute entangled regime.^{10,13,15} The entanglement concentration can be determined by plotting the Newtonian viscosity against the concentration on log–log scale.^{10,15} From the dilute to the semi-dilute unentangled regime, the viscosity curve changes from a linear (exponent typically 1)⁵⁹ to a power-law behavior, with an exponent higher than one.⁶⁰ From the semi-dilute unentangled regime on, the exponent of the power-law behavior is known to keep increasing, e.g., an exponent of 4 was reported for polyelectrolyte solutions.⁶¹ For all polymer–solvent combinations (Supporting Information, Figures S25–S40), the viscosity curve changes from a power law (exponent around 2) to a power-law behavior with a higher exponent (around 5). The dilute regime is not reached because this study focuses on the recommended concentrations for polymer solutions for the dissolution–precipitation technique (>5 wt %).⁸ The critical concentrations are in the range of 12.8–14.6 wt % and vary only slightly with temperature, as illustrated in Table 2.

Recalling that the recommended concentration for dissolution-based recycling is between 5 and 20 wt %, these results show that for concentrations higher than 15 wt %, the solutions enter the entangled semi-dilute regime, which might complicate cleaning steps during solvent-based recycling due to the drastic increase in viscosity. For example, for the PS/geranyl acetate case at 25 °C (Supporting Information, Figure S25), the viscosity of the 15 wt % is approximately four times the viscosity of the 10 wt % solution. It has been shown in a previous work by Kol et al.⁴ that for the dissolution–precipitation technique during the first cleaning steps, i.e., filtration of the polymer solution for removal of additives, an increase in polymer solution viscosity leads to a significant increase of the necessary pressure drop (to obtain the same flow rate). It can be also observed in Table 2 that *o*-xylene and anisole lead to the highest entanglement concentration, meaning that it is possible to dissolve a higher amount of polymer before entering the entangled region. Nonetheless, the

following results show that *o*-xylene results in a lower solution viscosity than anisole, and therefore, *o*-xylene can be used to maximize polymer concentration while minimizing the viscosity of the solution. Moreover, PS/limonene shows potential as an alternative to a conventional solvent, as it leads to a similar solution viscosity to *o*-xylene while its entanglement concentration does not significantly differ from *o*-xylene (0.3 wt % difference at 25 °C).

3.3.3. Influence of Solvent Type. The influence of the solvent on the polymer solution viscosity is presented in Figure 5 for 5 wt % solutions at 25 °C. The general trend shows that

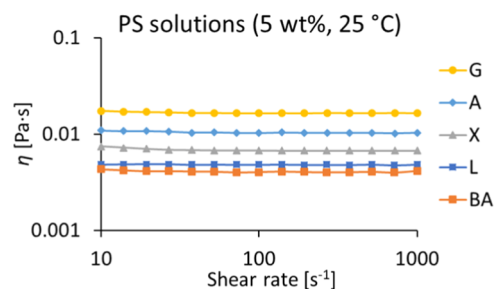


Figure 5. Influence of solvent type on the viscosity of flow curve for 5 wt % solution at 25 °C as an example. Abbreviations: G: geranyl acetate, A: anisole, X: *o*-xylene, L: limonene, and BA: *n*-butyl acetate.

geranyl acetate leads to the highest viscosities, followed by anisole, *o*-xylene, limonene, and *n*-butyl acetate at all temperatures and concentrations (Supporting Information, Figure S41). There is more of a direct relationship between the viscosity of the solvent and the viscosity of the solution rather more than the solvent type and solvation capacity. Polystyrene is a nonpolar polymer, meaning that the solvation capacity of nonpolar solvents is higher compared to polar ones. By comparing geranyl acetate (aprotic), *o*-xylene (nonpolar), and *n*-butyl acetate (aprotic), one observes that geranyl acetate, which leads to the highest viscosity of the solution, is also the solvent that has the highest viscosity (2.263 mPa·s at 25 °C). *o*-Xylene, a nonpolar solvent, leads, on the other hand, to a higher polymer solution viscosity than *n*-butyl acetate, which is a polar aprotic solvent. Looking at the viscosities of the pure solvents, *o*-xylene has a higher viscosity than *n*-butyl acetate, namely, 0.756 and 0.682 mPa·s at 25 °C, respectively (Spreadsheet File, Sheet 1). Thus, the viscosity of the solvent seems to have a higher influence on the viscosity of the solution compared to the solvent type and solvation capacity.

Overall, it can be concluded that the experimental data set for polymer solutions is dominated by Newtonian behavior, explaining the emphasis on Newtonian models in what follows.

3.4. From Experimental Data to Newtonian Viscosity Models. The Newtonian viscosities of the pure components are input for the Newtonian models involving dissolved polymers, and the results can be found in the Supporting Spreadsheet (Sheet 1). The models presented in Table S2 of the Supporting Information were applied to the different polymer solutions under different conditions, and these are the segment-based Eyring-NRTL (NRTL), segment-based Eyring-Wilson (Wilson), segment-based modified-NRF (mNRF), segment-based Eyring-NRF (NRF), and the polymer mixture viscosity model (PMV). For all models and polymer solutions, the experimentally determined viscosity of the pure components, solvent, and polymer, was used. In the Wilson model, the parameter that represents the effective coordination

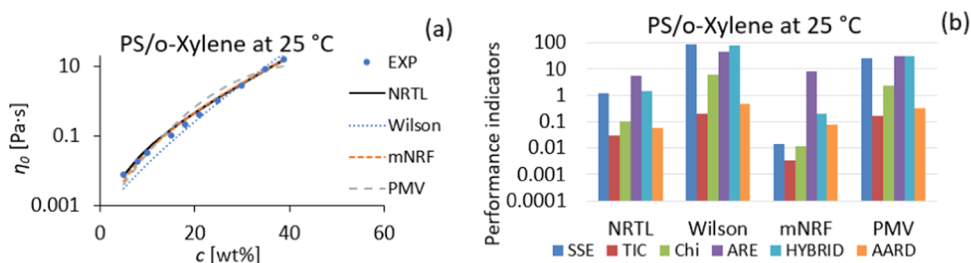


Figure 6. Fitting of the Newtonian models to PS/*o*-xylene solution at 25 °C (a) along with the corresponding performance indicators. (b) Newtonian viscosity fixed at 10 s⁻¹. The model SBNRF was excluded from the graph due to its large deviation.

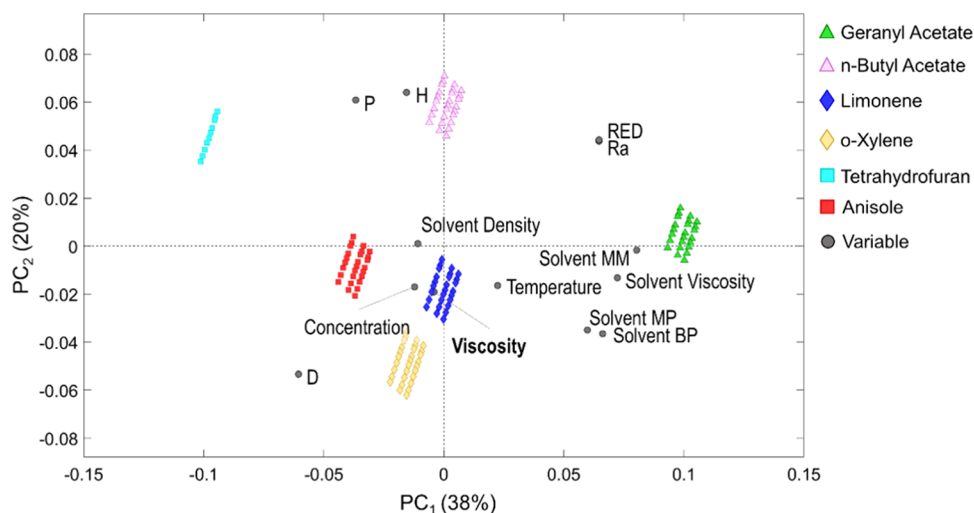


Figure 7. PCA biplot for polystyrene/solvent cases visualizing the relationship between samples and variables in the PC₁-PC₂ space.

number in the system, C_{Wilson} was fixed to 10.⁴⁸ The nonrandom factor of mNRF model, Z , was set to 8.⁵⁰

The results are presented in Figure 6 for PS/*o*-xylene at 25 °C. The other results can be found in the Supporting Information (Figures S42–S56). Generally, the models that best describe the viscosity of the different polymer solutions are the NRTL and mNRF models. This can be deduced from the performance indicators that show that these two models present the lowest values for all performance indicators (Supporting Information, Table S5). Looking at the obtained parameters (Supporting Information, Table S4) and focusing on the NRTL and mNRF models, the parameters vary with temperature and solvent type. For example, for the solution PS/geranyl acetate at 25 °C, the NRTL binary parameters, τ_{NRTL} are 147 and 44.2, and, at 50 °C, the parameters increase to 838 and 47.4, respectively. Therefore, these models are not suited to broader extrapolation and thus to other polymer–solvent systems and experimental conditions.

3.5. Strength of Multivariate Analysis. **3.5.1. Exploratory and Regression Analysis.** The first two principal components (PCs) were retained in the developed PCA model for exploratory analysis. The selected PCA model captures 58% of the variability in the data set, with the first and second PC capturing 38 and 20% of the variability (Figure 7). In a biplot, the scores of samples and loadings of variables are superimposed in one figure. The scores of samples can be used to inspect the relation between them. The scores show a clear grouping by solvent type. This was expected, as most of the included variables are properties of the solvent. However, there is no distinct grouping observed by solvent classification, e.g., a

grouping of all solutions in aprotic solvents. The loading of an original variable for a PC measures how much that variable contributes to that PC. The loadings for PC₁ and PC₂ were used to investigate how the original variables correlate to one another. If the relative positions of the variables in the scatter plot are close, this indicates that these variables might be correlated. This is the situation for the solvent properties molar mass (MM)/viscosity and boiling point (BP)/melting point (MP) and for properties regarding the affinity between the polymer and solvent, being RED/ R_a and P/H. On the loadings plot, the viscosity of the solution is found most related to the polymer concentration. This indicates the importance of concentration for predicting the viscosity of polymer solutions. RED/ R_a are found in the opposite quadrant of viscosity, indicating a negative correlation.

Based on the exploratory PCA analysis, eight independent variables were included upon building a partial least-squares (PLS) regression model to predict the viscosity of PS solutions. The variables in the model are solvent viscosity, density, melting point (MP), RED, polar cohesion (solubility) parameter, polymer concentration, and temperature. The first two latent variables (LVs) were retained in the PLS model. The selected PLS model captures 99% of the variability in viscosity of the different polymer solutions, with the first and second LV capturing 95 and 4% of the variability in viscosity based on respectively 10 and 32% of the variability in the independent variables. The final equation of the model includes all of these variables

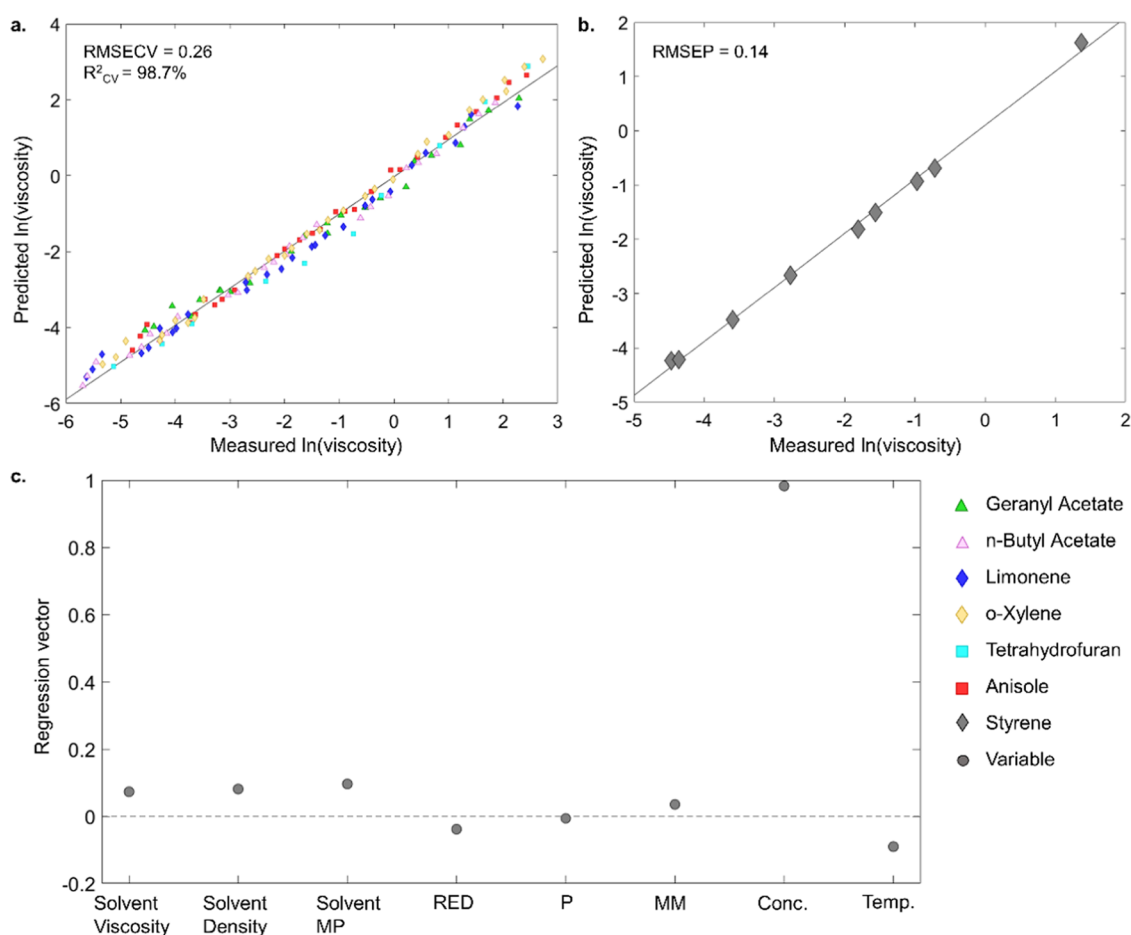


Figure 8. Results of the PLS model predicting the viscosity of PS solutions in new solvents—(a) Scatter plot of predicted and measured viscosities for samples in the calibration with a root-mean-square error of cross-validation (RMSECV) and the cross-validated coefficient of determination (R_{CV}^2), (b) scatter plot of predicted and measured viscosities for an external data set of PS solutions in the nonpolar solvent styrene with a root-mean-square error of prediction (RMSEP), and (c) regression vector for the developed PLS model.

Table 3. Validation Results for Two PLS Models to Predict the Viscosity of PS Solutions Based on Eight or Four Input Variables

regression method	regression coefficients									RMSECV	RMSEP
	$\ln(\eta_s)$	ρ_s	MP	RED	P	M	c	T	ε		
LR-1 Var							0.22		-5.83	0.53	0.17
MLR-2 Var							0.22	-0.015	-5.25	0.50	0.09
MLR-2 Var		0.0061					0.23		-11.27	0.43	0.09
MLR-3 Var		0.0058					0.23	-0.013	-10.56	0.40	0.10
PLS-4 Var		0.0046		0.91			0.23	-0.012	-10.21	0.39	0.16
PLS-8 Var	0.38	0.0038	0.0055	0.69	0.01	0.0024	0.23	-0.019	-8.00	0.26	0.14

$$\ln(\eta_0) = -8 + 0.38 \ln(\eta_s) + 0.0038\rho_s + 0.0055MP - 0.69RED - 0.01P + 0.0024MM + 0.23c - 0.019T + \varepsilon \quad (3)$$

where η_0 is the Newtonian viscosity of the solution [Pa·s], η_s is the solvent viscosity [mPa·s], ρ_s is the density of the solvent [$\text{kg}\cdot\text{m}^{-3}$], MP is the melting point of the solvent [$^{\circ}\text{C}$], RED is the relative energy difference from the HSP, P is the polar cohesion (solubility) parameter from HSP [$\text{MPa}^{1/2}$], MM is the molar mass of the solvent [$\text{g}\cdot\text{mol}^{-1}$], c is the concentration [wt %], T is temperature [$^{\circ}\text{C}$], and ε is the error [Pa·s].

Figure 8c shows the relative regression coefficients of the independent variables in the model. The polymer concen-

tration has the largest regression coefficient and has a positive contribution to the prediction of viscosity. Solvent viscosity, density, and MP each have a similar positive contribution. RED and polar cohesion (solubility) parameters have a marginal negative contribution. Finally, the temperature also has a negative contribution. The scatter plot of predicted and measured viscosities, as shown in Figure 8a, indicates that the model properly predicts the viscosity of samples in the calibration data set for different concentrations and temperatures. The model was also tested using an external validation data set with solutions of the nonpolar solvent styrene. The validation results in Figure 8 show that the PLS model accurately predicts the viscosity for styrene solutions, even though no solutions in styrene were included in the calibration

data. The M_w and dispersity of the molar mass distribution of polystyrene from the external data set ($M_w = 160\,000\text{ g}\cdot\text{mol}^{-1}$, $\bar{D} = 1.10$) also differs from the M_w of polystyrene used in the calibration data ($M_w = 265\,000\text{ g}\cdot\text{mol}^{-1}$, $\bar{D} = 2.65$). These results show the potential of multivariate data modeling to predict the viscosity of polymer solutions for different solvents at different temperatures and concentrations. In future research, this type of modeling can be applied to screen solvents by predicting the viscosity of its polymer solutions at different temperatures and concentrations without the need for additional extensive experimental work.

Furthermore, a series of simplified models were developed using one to four input variables and compared with the original model (eight variables). The validation results are given in Table 3. First, a linear regression model (LR-1 Var) predicting the viscosity of PS solutions based on only concentration was developed. Second, three multiple linear regression models (MLR) were tested, including concentration and either the variables' temperature, solvent density, or both. Finally, a simplified PLS model using one solvent property (density), one property related to the affinity between the polymer and the solvent (RED), temperature, and concentration was developed. It can be noted that the error after cross-validation for all simplified models is higher. However, due to their simplicity, the risk of overfitting is lower, and the simplified models may show to be more robust. Notably, the regression coefficient of concentration varies minimally (0.22–0.23) between the different models.

3.5.2. Comparison between Newtonian Viscosity Models.

The Newtonian viscosity models proposed in the literature are based on the conventional liquid mixture viscosity model and the addition of an excess term to account for nonlinearity. As shown above, these models are able to reasonably fit the experimental data under several conditions, including variations in temperature, concentration, and polymer–solvent system. However, different parameters were obtained for the individual polymer–solvent system and conditions. This means that the parameters are highly dependent on the system, and thus extrapolation of the viscosity to other systems and conditions is difficult or impossible. These models also require experimental data as input, for example, the viscosity of the pure components. If this data is unknown, then it can be treated as an adjustable parameter; however, this increases the number of adjustable parameters in the model, which can lead to overfitting. Nonetheless, these models can be suitable to predict the viscosity at different concentrations within one individual polymer–solvent system, for example, to predict the viscosity at a certain concentration that is difficult or was not experimentally determined.

The developed PLS model shows a great potential for predicting the viscosity of polystyrene solutions using statistical regression techniques. The validation of the model was performed with an external data set, which was a different polystyrene solution in a solvent that was not used to build the model. In addition, the polymer has a different average molar mass and dispersity than the polymers of the calibration data. This is very important for plastic recycling, as a typical plastic waste stream contains polymers with different average molar mass and dispersity. This thus poses an important advantage compared to the conventional application of the Newtonian viscosity models, consistent with the observation that the Newtonian viscosity model parameters can also be highly dependent on the average molar mass and dispersity of the

polymer.^{47,50} Furthermore, the PLS model does not require additional experimental data to extrapolate the viscosity to other polymer–solvent systems and experimental conditions, provided the initial training set is sufficiently large. Only the properties of the polymer–solvent system, such as temperature, polymer concentration, and solvent properties, are required, which simplifies the extrapolation, as shown above. In future research, the use of MVA for predicting the viscosity of other polymers should be studied and validated for polymer solutions of the same type but with other molar mass distribution and for other polymers besides PS to confirm its general applicability.

Hence, upon comparing both approaches, it can be stated that the prediction of the viscosity with the Newtonian viscosity models for solvent-based recycling has some limitations, especially due to the complexity of the plastic waste streams. MVA, on the other hand, has shown to be a promising alternative able to predict the viscosity of polystyrene solutions regardless of the experimental conditions and polymer–solvent system properties. This is relevant in solvent-based recycling, where different solvents and anti-solvents are used in several steps of the process. Moreover, for the selective dissolution of polymers, where different experimental conditions and polymer–solvent systems are in play, MVA could simplify the prediction of several polymer solutions' viscosity for the optimization of the process.

4. CONCLUSIONS

A systematic analysis of the rheological behavior of polymer solutions under different conditions has been performed. The results show that polystyrene solutions at different conditions of temperature, concentration, and solvent type, show mainly Newtonian behavior in the studied shear rate range of 1–1000 s^{-1} . High concentrations of polymer lead to more viscous solutions, whereas an increase in temperature decreases the viscosity of the solutions. It has also been shown that the solvent type and properties influence the viscosity of polymer solutions, with *n*-butyl acetate leading to the lowest solution viscosity and geranyl acetate to the highest at all temperatures (25–50 °C) and concentrations (5–39 wt %) studied. The entanglement concentration of all polymer solutions was determined, being in the range of 12.8–14.6 wt %. Above this concentration, the polymer solutions enter an entangled semi-dilute regime, where polymer entanglements start to form, leading to a drastic increase in viscosity. Furthermore, limonene shows potential as an alternative to a conventional solvent, as it leads to a similar solution viscosity to *o*-xylene.

The Newtonian viscosity of the polymer solutions was described with Newtonian viscosity models from the literature, and a partial least-squares regression model was considered to predict the viscosity of the polymer solutions. The segment-based Eyring-NRTL and modified-NRF are the models that best describe the Newtonian viscosity of polymer solutions under different conditions. However, it has been shown that the obtained model parameters are highly dependent on the system and thus extrapolation of the viscosity to other systems and conditions is difficult or impossible. To overcome this, a multivariate data analysis was performed as well. The results show that the developed partial least-squares regression model can reasonably predict the viscosity of polymer solutions regardless of the experimental conditions and polymer–solvent system properties. This is especially relevant in solvent-based recycling techniques for plastic waste streams, where the waste

composition is variable and complex, and several solvents are used in different steps of the cleaning process. In future research, it is interesting to apply and validate these models to other polymers solutions beyond the polystyrene reference polymer choice. In addition, a hybrid approach could be investigated, combining both physical and statistical modeling, to further improve the predictive power and general applicability of the developed models.

■ ASSOCIATED CONTENT

SI Supporting Information

The Supporting Information is available free of charge at <https://pubs.acs.org/doi/10.1021/acs.iecr.2c01487>.

Appendix A. Supporting Information: screening of solvents–HSP analysis, calculation of TGA error, Newtonian viscosity models, solubility limits of polymer solutions, viscosity of polymer solutions, Newtonian viscosity model fitting (PDF)

Appendix B. Supporting Spreadsheet: experimental data (XLSX)

■ AUTHOR INFORMATION

Corresponding Author

Steven De Meester – Laboratory for Circular Process Engineering (LCPE), Department of Green Chemistry and Technology, Ghent University, 8500 Kortrijk, Belgium; orcid.org/0000-0002-5246-3918; Email: Steven.DeMeester@UGent.be

Authors

Rita Kol – Laboratory for Circular Process Engineering (LCPE), Department of Green Chemistry and Technology, Ghent University, 8500 Kortrijk, Belgium; Laboratory of Polymer Chemistry and Technology, Department of Chemistry, Aristotle University of Thessaloniki, 54124 Thessaloniki, Greece; orcid.org/0000-0003-1542-7085

Pieter Nachtergaele – Research Group STEN, Department of Green Chemistry & Technology, Ghent University, B-9000 Ghent, Belgium

Tobias De Somer – Laboratory for Circular Process Engineering (LCPE), Department of Green Chemistry and Technology, Ghent University, 8500 Kortrijk, Belgium

Dagmar R. D'hooge – Laboratory for Chemical Technology (LCT) and Centre for Textiles Science and Engineering (CTSE), Department of Materials, Textiles and Chemical Engineering, Faculty of Engineering and Architecture, Ghent University, 9052 Zwijnaarde, Belgium; orcid.org/0000-0001-9663-9893

Dimitris S. Achilias – Laboratory of Polymer Chemistry and Technology, Department of Chemistry, Aristotle University of Thessaloniki, 54124 Thessaloniki, Greece; orcid.org/0000-0003-2872-8426

Complete contact information is available at: <https://pubs.acs.org/doi/10.1021/acs.iecr.2c01487>

Author Contributions

R.K.: Conceptualization, methodology, validation, software, investigation, visualization, writing—original draft. P.N.: Software, writing—original draft (Chapter 2.5.2 and 3.5.1), writing—review and editing. T.D.S.: Software, writing—review and editing. D.R.D.: Visualization, writing—review, and editing. D.S.A.: Writing—review and editing. S.D.M.: Conceptualiza-

tion, resources, visualization, writing—review and editing, supervision, project administration, and funding acquisition.

Notes

The authors declare no competing financial interest.

■ ACKNOWLEDGMENTS

This work was financially supported by the C-PlaNeT (Circular Plastics Network for Training) project from the European Union's Horizon 2020 research and innovation program (Marie Skłodowska-Curie Grant Agreement No. 859885) and by the Catalisti-Moonshot project Renovate granted by the Vlaams Agentschap Innoveren & Ondernemen (VLAIO).

■ REFERENCES

- (1) Song, Y.; Mathias, P. M.; Tremblay, D.; Chen, C. C. Liquid Viscosity Model for Polymer Solutions and Mixtures. *Ind. Eng. Chem. Res.* **2003**, *42*, 2415–2422.
- (2) D'Hooge, D. R.; Van Steenberge, P. H. M.; Reyniers, M. F.; Marin, G. B. The Strength of Multi-Scale Modeling to Unveil the Complexity of Radical Polymerization. *Prog. Polym. Sci.* **2016**, *58*, 59–89.
- (3) De Keer, L.; Kilic, K. I.; Van Steenberge, P. H. M.; Daelemans, L.; Kodura, D.; Frisch, H.; De Clerck, K.; Reyniers, M. F.; Barner-Kowollik, C.; Dauskardt, R. H.; D'hooge, D. R. Computational Prediction of the Molecular Configuration of Three-Dimensional Network Polymers. *Nat. Mater.* **2021**, *20*, 1422–1430.
- (4) Kol, R.; Somer, T.; De D'hooge, D. R.; Knappich, F.; Ragaert, K.; Achilias, D. S.; De Meester, S. State-of-the-Art on Quantification of Polymer Solution Viscosity for Plastic Waste Recycling. *ChemSusChem* **2021**, *14*, 4071–4102.
- (5) Kol, R.; Roosen, M.; Ügdüler, S.; M Van Geem, K.; Ragaert, K.; S Achilias, D.; De Meester, S. Recent Advances in Pre-Treatment of Plastic Packaging Waste. In *Waste Material Recycling in the Circular Economy - Challenges and Developments*; Achilias, S. D., Ed.; IntechOpen, 2021.
- (6) Ügdüler, S.; Van Geem, K. M.; Roosen, M.; Delbeke, E. I. P.; De Meester, S. Challenges and Opportunities of Solvent-Based Additive Extraction Methods for Plastic Recycling. *Waste Manag.* **2020**, *104*, 148–182.
- (7) Walker, T. W.; Frelka, N.; Shen, Z.; Chew, A. K.; Banick, J.; Grey, S.; Kim, M. S.; Dumesic, J. A.; Van Lehn, R. C.; Huber, G. W. Recycling of Multilayer Plastic Packaging Materials by Solvent-Targeted Recovery and Precipitation. *Sci. Adv.* **2020**, *6*, No. eaba7599.
- (8) Nauman, E. B.; Lynch, J. C. Polymer Recycling by Selective Dissolution. U.S. Patent US5,278,282, 1994.
- (9) Notari, M.; Rivetti, F. Use of Dialkyl Carbonates as Solvents for Expanded Polystyrene. U.S. Patent US7,745,503, 2010.
- (10) Agasty, A.; Wisniewska, A.; Kalwarczyk, T.; Koynov, K.; Holyst, R. Scaling Equation for Viscosity of Polydimethylsiloxane in Ethyl Acetate: From Dilute to Concentrated Solutions. *Polymer* **2020**, *203*, No. 122779.
- (11) Ren, L.; Pandit, V.; Elkin, J.; Denman, T.; Cooper, J. A.; Kotha, S. P. Large-Scale and Highly Efficient Synthesis of Micro- and Nano-Fibers with Controlled Fiber Morphology by Centrifugal Jet Spinning for Tissue Regeneration. *Nanoscale* **2013**, *5*, 2337–2345.
- (12) Van Krevelen, D. W.; Te Nijenhuis, K. *Properties of Polymers: Their Correlation with Chemical Structure; Their Numerical Estimation and Prediction from Additive Group Contributions*, 4th ed.; Elsevier B.V., 2009.
- (13) El Aferni, A.; Guettari, M.; Kamli, M.; Tajouri, T.; Ponton, A. A Structural Study of a Polymer-Surfactant System in Dilute and Entangled Regime: Effect of High Concentrations of Surfactant and Polymer Molecular Weight. *J. Mol. Struct.* **2020**, *1199*, No. 127052.
- (14) Wiśniewska, A.; Sozański, K.; Kalwarczyk, T.; Kędra-Królik, K.; Pieper, C.; Wiczorek, S. A.; Jakiela, S.; Enderlein, J.; Holyst, R. Scaling of Activation Energy for Macroscopic Flow in Poly(Ethylene

- Glycol) Solutions: Entangled - Non-Entangled Crossover. *Polymer* **2014**, *55*, 4651–4657.
- (15) Haro-Pérez, C.; Andablo-Reyes, E.; Díaz-Leyva, P.; Arauz-Lara, J. L. Microrheology of Viscoelastic Fluids Containing Light-Scattering Inclusions. *Phys. Rev. E* **2007**, *75*, No. 041505.
- (16) Barnes, H. A. *A Handbook of Elementary Rheology*; University of Wales Institute of Non-Newtonian Fluid Mechanics, Department of Mathematics, University of Wales Aberystwyth: Aberystwyth, 2000.
- (17) Marani, D.; Gadea, C.; Hjelm, J.; Hjalmarsson, P.; Wandel, M.; Kiebach, R. Influence of Hydroxyl Content of Binders on Rheological Properties of Cerium-Gadolinium Oxide (CGO) Screen Printing Inks. *J. Eur. Ceram. Soc.* **2015**, *35*, 1495–1504.
- (18) Osswald, T.; Rudolph, N. *Polymer Rheology, Fundamentals and Applications*; Strohm, C., Ed.; Carl Hanser Verlag: Munich, 2015.
- (19) Konstantinov, I.; Villa, C.; Cong, R.; Karjala, T. Viscosity Modeling of Polymer Solutions. *Macromol. Symp.* **2018**, *377*, No. 1600179.
- (20) Nishimura, N. Viscosities of Concentrated Polymer Solutions. *J. Polym. Sci., Part A: Gen. Pap.* **1965**, *3*, 237–253.
- (21) Kim, D. M.; Nauman, E. B. Solution Viscosity of Polystyrene at Conditions Applicable to Commercial Manufacturing Processes. *J. Chem. Eng. Data* **1992**, *37*, 427–432.
- (22) Ottani, S.; Vitalini, D.; Comelli, F.; Castellari, C. Densities, Viscosities, and Refractive Indices of Poly(Ethylene Glycol) 200 and 400 + Cyclic Ethers at 303.15 K. *J. Chem. Eng. Data* **2002**, *47*, 1197–1204.
- (23) Pezzin, G.; Gligo, N. Viscosity of Concentrated Polymer Solutions. I. Polyvinylchloride in Cyclohexanone. *J. Appl. Polym. Sci.* **1966**, *10*, 1–19.
- (24) Kinzl, M.; Luft, G.; Horst, R.; Wolf, B. A. Viscosity of Solutions of Low-Density Polyethylene in Ethylene as a Function of Temperature and Pressure. *J. Rheol.* **2003**, *47*, 869–877.
- (25) Ehrlich, P.; Woodbrey, J. C. Viscosities of Moderately Concentrated Solutions of Polyethylene in Ethane, Propane, and Ethylene. *J. Appl. Polym. Sci.* **1969**, *13*, 117–131.
- (26) Nachtergaele, P.; Thybaut, J.; De Meester, S.; Drijvers, D.; Saeyns, W.; Dewulf, J. Multivariate Analysis of Industrial Biorefinery Processes: Strategy for Improved Process Understanding with Case Studies in Fatty Acid Production. *Ind. Eng. Chem. Res.* **2020**, *59*, 7732–7745.
- (27) Wu, Y. Y.; Figueira, F. L.; Edeleva, M.; Van Steenberge, P. H. M.; D'hooge, D. R.; Zhou, Y. N.; Luo, Z. H. Cost-Efficient Modeling of Distributed Molar Mass and Topological Variations in Graft Copolymer Synthesis by Upgrading the Method of Moments. *AIChE J.* **2022**, *68*, No. e17559.
- (28) Ramos, P. F. d. O.; de, O.; de Toledo, I. B.; Nogueira, C. M.; Novotny, E. H.; Vieira, A. J. M.; Azeredo, R. B.; de, V. Low Field 1H NMR Relaxometry and Multivariate Data Analysis in Crude Oil Viscosity Prediction. *Chemom. Intell. Lab. Syst.* **2009**, *99*, 121–126.
- (29) Petersen, N.; Stocks, S.; Gernaey, K. V. Multivariate Models for Prediction of Rheological Characteristics of Filamentous Fermentation Broth from the Size Distribution. *Biotechnol. Bioeng.* **2008**, *100*, 61–71.
- (30) Sato, A. C. K.; Oliveira, P. R.; Cunha, R. L. Rheology of Mixed Pectin Solutions. *Food Biophys.* **2008**, *3*, 100–109.
- (31) Mohammadi, M.; Khorrami, M. K.; Ghasemzadeh, H. ATR-FTIR Spectroscopy and Chemometric Techniques for Determination of Polymer Solution Viscosity in the Presence of SiO₂ Nanoparticle and Salinity. *Spectrochim. Acta, Part A* **2019**, *220*, No. 117049.
- (32) Donoso, M.; Ghaly, E. S. Use of Near-Infrared for Quantitative Measurement of Viscosity and Concentration of Active Ingredient in Pharmaceutical Gel. *Pharm. Dev. Technol.* **2006**, *11*, 389–397.
- (33) Yousefi, F.; Karimi, H.; Mohammadian, S. Viscosity of Carbon Nanotube Suspension Using Artificial Neural Networks with Principal Component Analysis. *Heat Mass Transf.* **2016**, *52*, 2345–2355.
- (34) Oh, C. M.; Heng, P. W. S.; Chan, L. W. A Study on the Impact of Hydroxypropyl Methylcellulose on the Viscosity of PEG Melt Suspensions Using Surface Plots and Principal Component Analysis. *AAPS PharmSciTech* **2015**, *16*, 466–477.
- (35) Pacheco-Fernández, I.; Pino, V. Green Solvents in Analytical Chemistry. *Curr. Opin. Green Sustainable Chem.* **2019**, *18*, 42–50.
- (36) García, M. T.; Duque, G.; Gracia, I.; De Lucas, A.; Rodríguez, J. F. Recycling Extruded Polystyrene by Dissolution with Suitable Solvents. *J. Mater. Cycles Waste Manag.* **2009**, *11*, 2–5.
- (37) Sun, C.; Theodoropoulos, C.; Scrutton, N. S. Techno-Economic Assessment of Microbial Limonene Production. *Bioresour. Technol.* **2020**, *300*, No. 122666.
- (38) Jongedijk, E.; Cankar, K.; Buchhaupt, M.; Schrader, J.; Bouwmeester, H.; Beekwilder, J. Biotechnological Production of Limonene in Microorganisms. *Appl. Microbiol. Biotechnol.* **2016**, *100*, 2927–2938.
- (39) Jahandideh, A.; Johnson, T. J.; Esmaeili, N.; Johnson, M. D.; Richardson, J. W.; Muthukumarappan, K.; Anderson, G. A.; Halfmann, C.; Zhou, R.; Gibbons, W. R. Life Cycle Analysis of a Large-Scale Limonene Production Facility Utilizing Filamentous N₂-Fixing Cyanobacteria. *Algal Res.* **2017**, *23*, 1–11.
- (40) Cheng, S.; Liu, X.; Jiang, G.; Wu, J.; Zhang, J. L.; Lei, D.; Yuan, Y. J.; Qiao, J.; Zhao, G. R. Orthogonal Engineering of Biosynthetic Pathway for Efficient Production of Limonene in *Saccharomyces Cerevisiae*. *ACS Synth. Biol.* **2019**, *8*, 968–975.
- (41) Hanson, C. D.; Burrell, T.; Haworth, J. E.; Olson, J. A. Pyrolysis Method for Increasing Limonene Production and Novel Oven to Facilitate Such Method. U.S. Patent US6,149,881, 2000.
- (42) Januszewicz, K.; Kazimierski, P.; Suchocki, T.; Kardaś, D.; Lewandowski, W.; Klugmann-Radziemska, E.; Łuczak, J. Waste Rubber Pyrolysis: Product Yields and Limonene Concentration. *Materials* **2020**, *13*, No. 4435.
- (43) Danon, B.; Van Der Gryp, P.; Schwarz, C. E.; Görgens, J. F. A Review of Dipentene (DL-Limonene) Production from Waste Tire Pyrolysis. *J. Anal. Appl. Pyrolysis* **2015**, *112*, 1–13.
- (44) Hansen, C. M. *Hansen Solubility Parameters: A User's Handbook*, 2nd ed.; CRC Press, Taylor & Francis Group, LLC: Boca Raton, 2007.
- (45) Gutiérrez, C.; García, M. T.; Gracia, I.; De Lucas, A.; Rodríguez, J. F. The Selective Dissolution Technique as Initial Step for Polystyrene Recycling. *Waste Biomass Valorization* **2013**, *4*, 29–36.
- (46) Achilias, D. S.; Giannoulis, A.; Papageorgiou, G. Z. Recycling of Polymers from Plastic Packaging Materials Using the Dissolution-Reprecipitation Technique. *Polym. Bull.* **2009**, *63*, 449–465.
- (47) Novak, L. T.; Chen, C. C.; Song, Y. Segment-Based Eyring-NRTL Viscosity Model for Mixtures Containing Polymers. *Ind. Eng. Chem. Res.* **2004**, *43*, 6231–6237.
- (48) Sadeghi, R. Segment-Based Eyring-Wilson Viscosity Model for Polymer Solutions. *J. Chem. Thermodyn.* **2005**, *37*, 445–448.
- (49) Sadeghi, R. Modification of the Nonrandom Factor (NRF) Model for Correlation of the Viscosity of Polymer Solutions. *Fluid Phase Equilib.* **2005**, *232*, 70–73.
- (50) Zafarani-Moattar, M. T.; Majdan-Cegincara, R. New Excess Gibbs Energy Equation for Modeling the Thermodynamic and Transport Properties of Polymer Solutions and Nanofluids at Different Temperatures. *Ind. Eng. Chem. Res.* **2011**, *50*, 8245–8262.
- (51) Abdi, H. Partial Least Squares Regression and Projection on Latent Structure Regression (PLS Regression). *Wiley Interdiscip. Rev.: Comput. Stat.* **2010**, *2*, 97–106.
- (52) Ferreira, A. P.; Tobyn, M. Multivariate Analysis in the Pharmaceutical Industry: Enabling Process Understanding and Improvement in the PAT and QbD Era. *Pharm. Dev. Technol.* **2015**, *20*, 513–527.
- (53) Kjeldahl, K.; Bro, R. Some Common Misunderstandings in Chemometrics. *J. Chemom.* **2010**, *24*, 558–564.
- (54) Aptula, A. O.; Jeliakova, N. G.; Schultz, T. W.; Cronin, M. T. D. The Better Predictive Model: High Q₂ for the Training Set or Low Root Mean Square Error of Prediction for the Test Set? *QSAR Comb. Sci.* **2005**, *24*, 385–396.
- (55) Eriksson, L.; Byrne, T.; Johansson, E.; Trygg, J.; Vikström, C. *Multi- and Megavariate Data Analysis, Basic Principles and Applications*, 3rd ed.; Umetrics Academy: Malmö, 2013.

(56) Qin, J.; Milner, S. T. Tubes, Topology, and Polymer Entanglement. *Macromolecules* **2014**, *47*, 6077–6085.

(57) Klein, J. The Onset of Entangled Behavior in Semidilute and Concentrated Polymer Solutions. *Macromolecules* **1978**, *11*, 852–858.

(58) Carnicer, V.; Alcázar, C.; Orts, M. J.; Sánchez, E.; Moreno, R. Microfluidic Rheology: A New Approach to Measure Viscosity of Ceramic Suspensions at Extremely High Shear Rates. *Open Ceram.* **2021**, *5*, No. 100052.

(59) Morris, E. R.; Cutler, A. N.; Ross-Murphy, S. B.; Rees, D. A.; Price, J. Concentration and Shear Rate Dependence of Viscosity in Random Coil Polysaccharide Solutions. *Carbohydr. Polym.* **1981**, *1*, 5–21.

(60) Rayner, M.; Östbring, K.; Purhagen, J. Application of Natural Polymers in Food. In *Natural Polymers*; Olatunji, O., Ed.; Springer International Publishing Switzerland: Switzerland, 2016; pp 115–161.

(61) Velazquez-garcia, A.; Rivera-vallejo, C.; Cadenas-pliego, G.; Pérez-alvarez, M.; De, R. D.; Jiménez-regalado, E. Synthesis, Characterization and Rheological Properties of Telechelic Polyelectrolytes. *Rev. Téc. Ing. Univ. Zulia. Vol.* **2015**, *38*, 69–79.